Electronic Supplementary Material (ESI) for Nanoscale.

Supporting Information for "Plasmon-enhanced versatile optical nonlinearities in Au-Ag-Au multi-segmental hybrid structure"

Linhua Yao,[1] Junpei Zhang,[1] Hongwei Dai,[1] Mingshan Wang,[1] Luman Zhang,[1] Xia Wang,[2] Jun-Bo Han[1,*]

[1]Wuhan National High Magnetic Field Center and School of Physics, Huazhong University of Science and Technology, Wuhan 430074, China.

[2]School of Mathematics and Physics, Wenhua College, Wuhan 430074, PR China

*Email：junbo.han@mail.hust.edu.cn

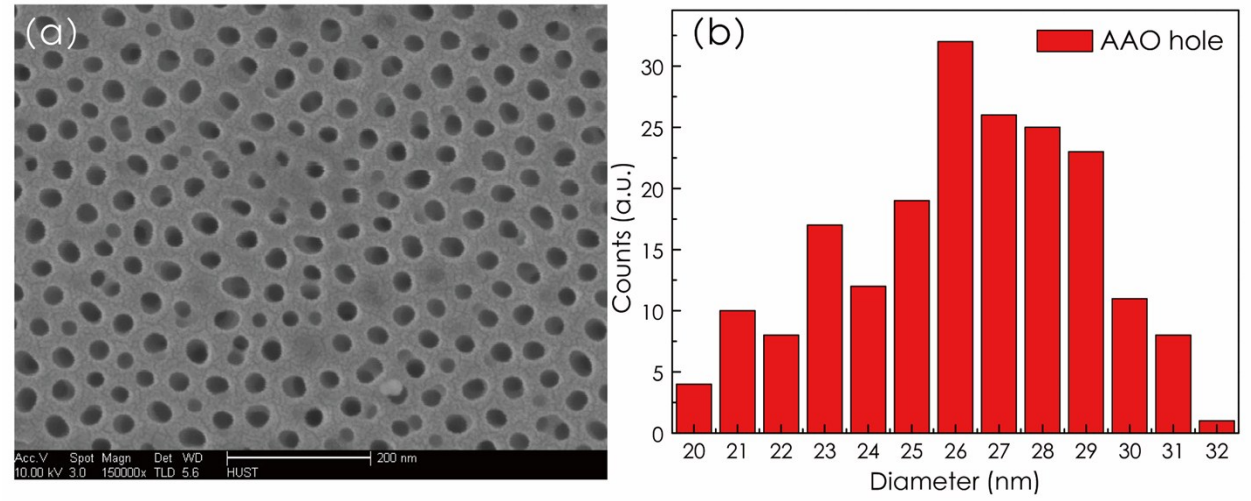

Figure S1. (a) Top-view SEM image of the whole AAO membrane. (b) The diameter distribution of the AAO holes. The holes are extracted from (a).

Fig. S1(a) shows a larger area of AAO image than that given in Fig. 1(b), and the Fig. S1 gives the statistical data of the diameter of the AAO holes. As shown in Fig. S1(b), the main diameter of the AAO holes are from 23 nm to 29 nm. Hence, the average diameter of the holes is 26 ± 3 nm. In our work, the ~30 μm diameter beam spot is much larger than the nanorods diameter, hundreds of thousands of nanorods were excited by the laser beam. The observed nonlinear signals represent the average performance of nanorods hybrid structure film systems which helped us to minimize signals' deviations from variations of individual nanorod. Therefore, the variations of individual nanorod is acceptable.

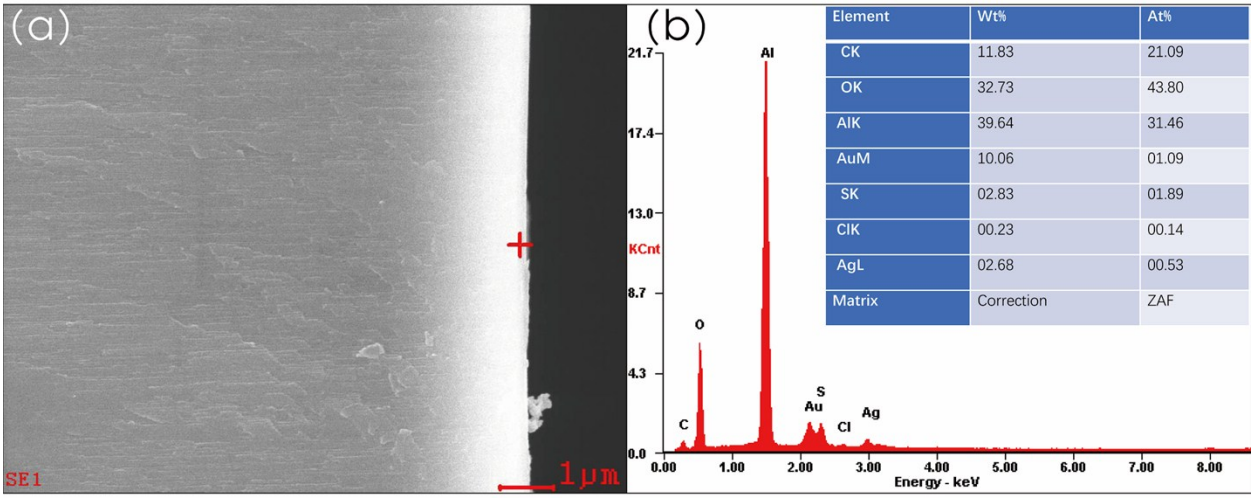

Figure S2. Point EDAX element analysis of Au-Ag-Au hybrid structure. (a) Cross-section image of the sample with EDAX measurement location marked with a red cross point. (b) EDAX spectrum taken at the marked point, the inset gives the content ratio of different element. Both Au and Ag elements could be observed from the spectrum.

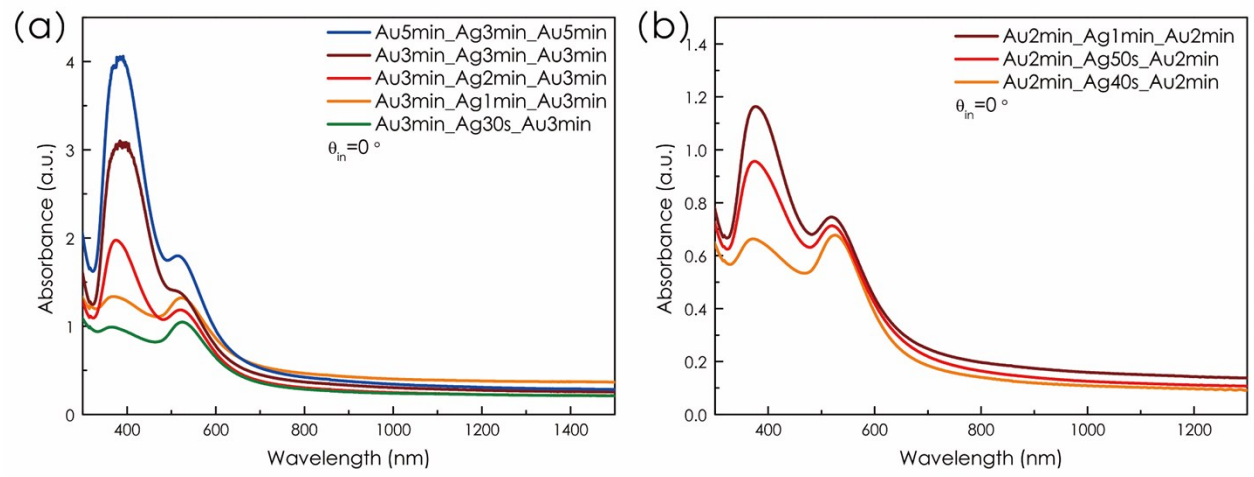

Figure S3. The absorbance spectra Au-Ag-Au nanorod hybrid structures with different Au and Ag deposition times. The incident light angle is 0 degree.

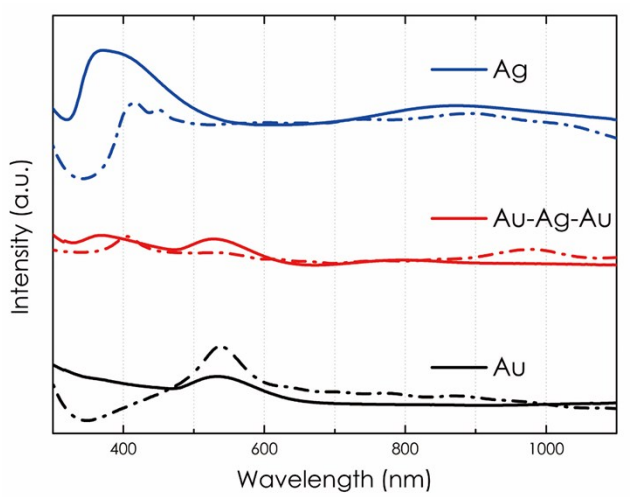

Figure S4. The simulated absorption spectra (dashed line) of Au, Ag and Au-Ag-Au nanorods hybrid structures together with the experimental ones. In the simulation, the nanorods are assumed to be round and homogenous, and only one nanorod was selected during the simulation for simplification. The profiles of simulated absorption curves agree well with the experimental ones.

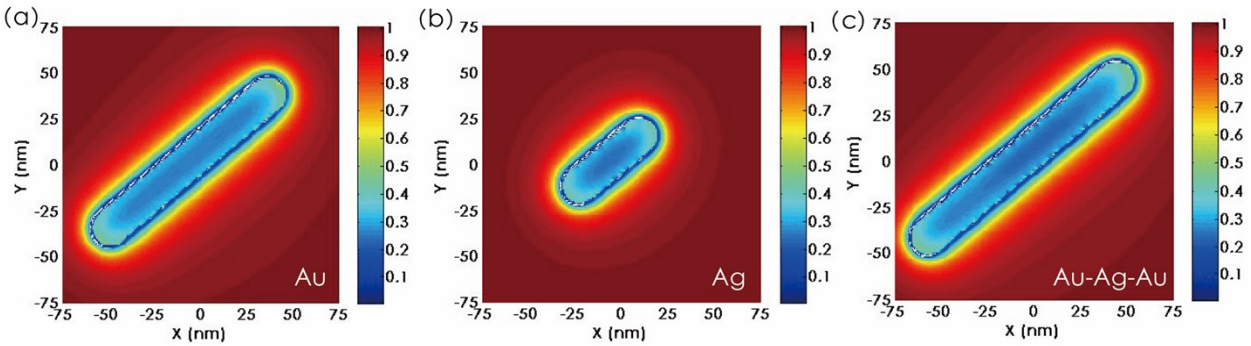

Figure S5. Calculated electric-field distribution of Au, Au, and Au-Ag-Au nanorods under *s*-polarized laser excitation at 800 nm. The electric field intensity *E* is nearly 1 for all nanorods under *s*-polarized laser excitation.

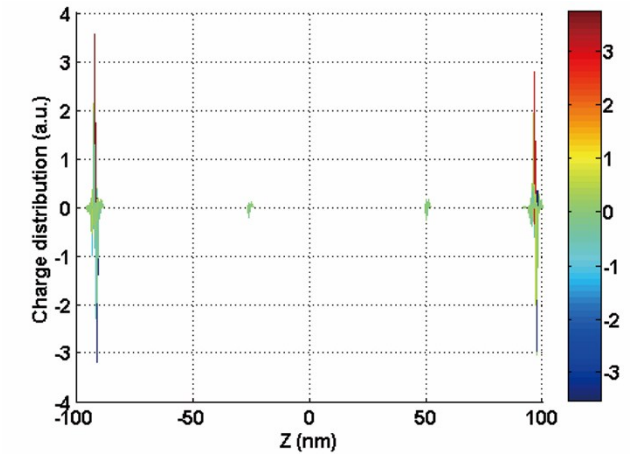

Figure S6. The charge density distribution of Au-Ag-Au nanorod. The figure was plotted under side view direction for better revealing the charge distribution between the Au and Ag interface.

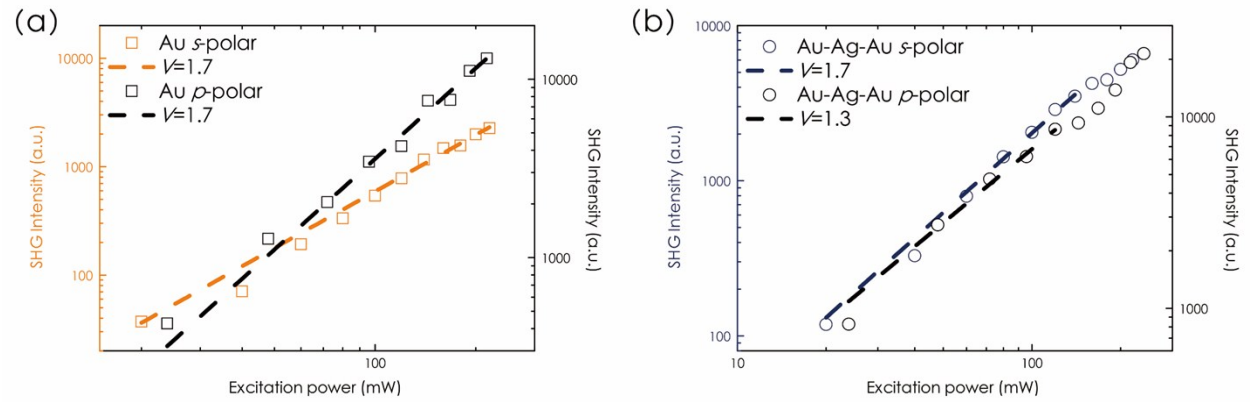

Figure S7. Peak SHG intensities of Au (a) and Au-Ag-Au (b) nanorod hybrid structures versus the excitation power. The hollow dots are experimental data while the lines are linear fittings. The slopes are much smaller than 2.

S8. The qualitative interpretation of the SHG intensity of Ag nanorod hybrid structure is larger than Au-Ag-Au sample.

Plasmon enhanced SHG intensity can be approximately given as[1, 2] $I_{SHG} \propto L_{(\omega)}^4 \cdot L_{(2\omega)}^2$, where $L_{(\omega)}$ refers to the local field enhancement through $L_{(\omega)} = E_{loc(\omega)}/E_{(\omega)}$. $E_{loc(\omega)}$ and $E_{(\omega)}$ are the localized electric field and the incident electric field at excitation frequency. $L_{(2\omega)}$ refers to the local field enhancement at second harmonic frequency. Hence, both LSPR and TSPR have contributions to local field enhancements of Ag and Au-Ag-Au samples.

Two main reasons cause the SHG intensity of Ag nanorod hybrid structure is larger than Au-Ag-Au sample. The first one is, for Au-Ag-Au sample, partial excitation energy converts into PL which decreases the absorbed plasmon energy at excitation frequency (ω) for converting into second harmonic generation. The second one is, the $L_{(2\omega)}$ of Ag sample is larger than Au-Ag-Au sample as the FDTD simulation results demonstrated below. Therefore, it is reasonable that the measured Plasmon-enhanced SHG intensity of Ag nanorod hybrid structure is larger than that of Au-Ag-Au sample.

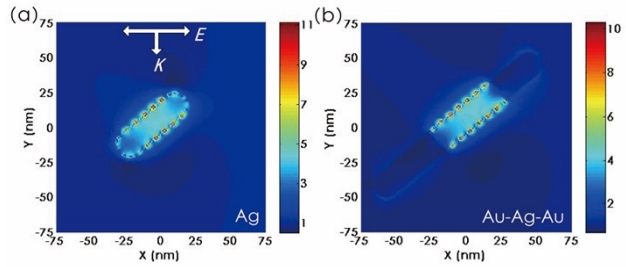

Figure S8. Calculated electric-field distribution of Ag (a) and Au-Ag-Au (b) nanorods at second harmonic frequency (400 nm) under *p*-polarized excitation.

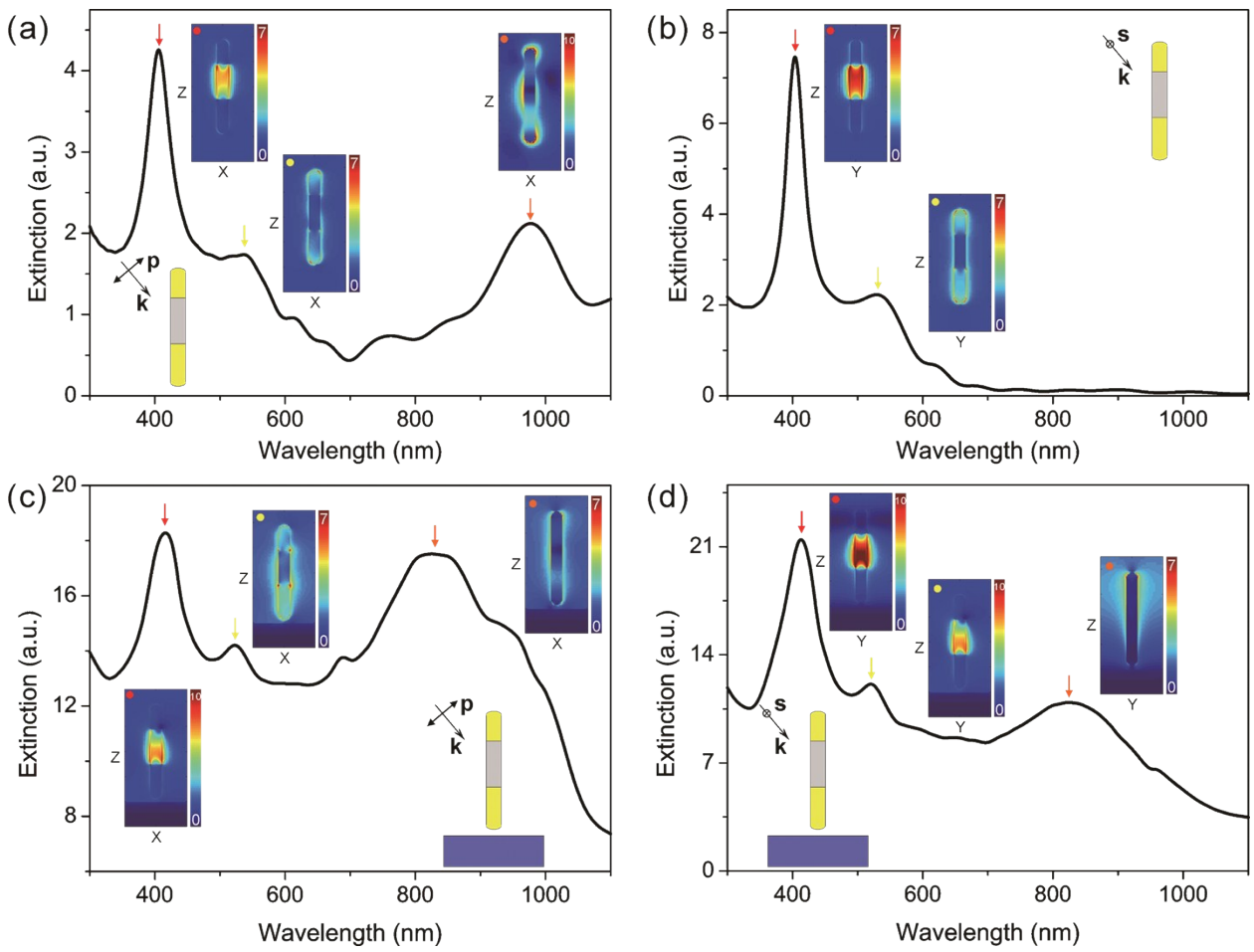

Figure S9. Calculated extinction spectra of the fabricated Au-Ag-Au nanorod with or without the Al substrate. (a) *p*-polarization and (b) *s*-polarization without substrate, (c) *p*-polarization and (b) *s*-polarization with substrate. The radius of the rod is 9 nm, the length is 40-55-55 nm, the surrounding medium is Al_2O_3 (n = 1.76), the separation with the Al substrate is 6 nm, the incident angle is 40 degrees, and the insets are the near-field enhancement distributions of the main resonances.

Fig. S9 shows the calculated extinction spectra of a single Au-Ag-Au nanorod under oblique incidence with/without the Al substrate. When the substrate is removed (Figure S9 a and b), pronounced resonances around 410 and 520 nm are observed for both *p*- and *s*-polarized incidences, which agree well with the measured spectra shown in Figure 2. According to the near-field distributions shown in the insets, the two resonances are caused by the excitation of the transverse LSPs of the Ag and Au rod, respectively. Besides that, there is a resonance around 980 nm that can only be effectively excited with the *p*-polarized incidence, which is related to the excitation a multipolar mode of the nanorod. For the nanorod with the substrate (Figure S9 c and d), the two resonances around 410 and 520 nm are not strongly affected with the present of the Al film, and the coupling with the substrate is weak. In addition, a resonance at about 820 nm appears in both spectra. The near-field distribution of the resonance with the *p*-polarized incidence is relatively complex, which is related to the excitation of the multipolar and dipole modes of the nanorod. For the s-polarized incidence, the near-field distribution indicate that the resonance is caused by the excitation of a collective dipole mode of the whole nanorod. Recently, Chen et al. have demonstrated that a magnetic resonance can be excited when a gold nanosphere is placed on a metallic film, and strong magnetic fields are generated around the gap area.[3] The fabricated nanorods in our study are also placed on a metallic film when the Al substrate is not removed. However, the separation between the rod and substrate is relatively large, and the nanorods are perpendicularly oriented against the substrate. As a result, the coupling with substrate is weak, and the magnetic resonance is not effectively excited in our case.

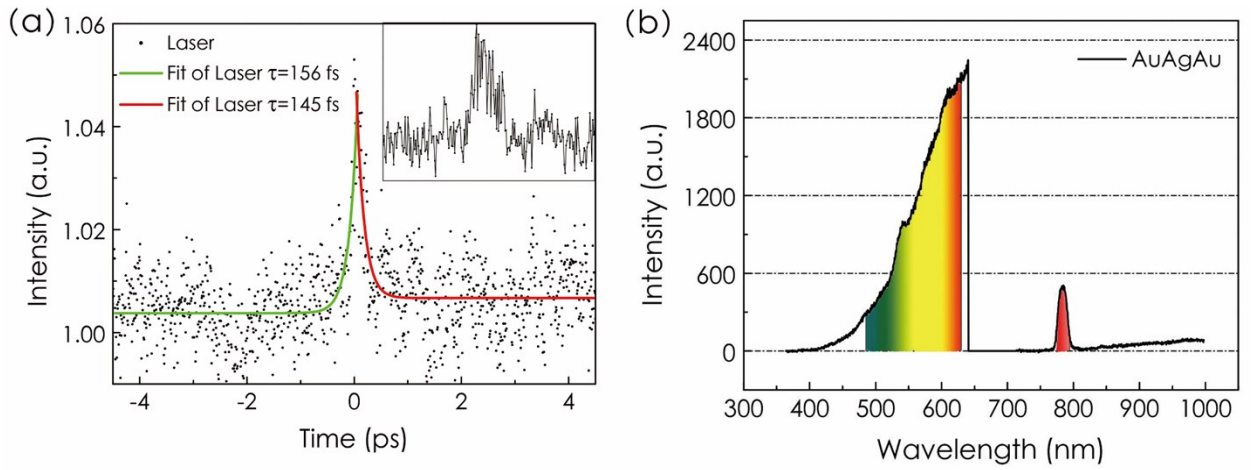

Figure S10. (a) Normalized time-resolved PL for the scattering laser. Each data point was obtained from the integration of the scattering laser spectrum from 775 nm to 795 nm. The solid lines are fitting curves by using a single exponential function. The decay time is exacted to be 156 (145) fs. The inset indicates the interference of the laser pulses. (b) A typical PL spectra of Au-Ag-Au nanorod hybrid structure. The color region from 486 nm to 630 nm (775 nm to 795 nm) is selected integration of SC (laser) signal.

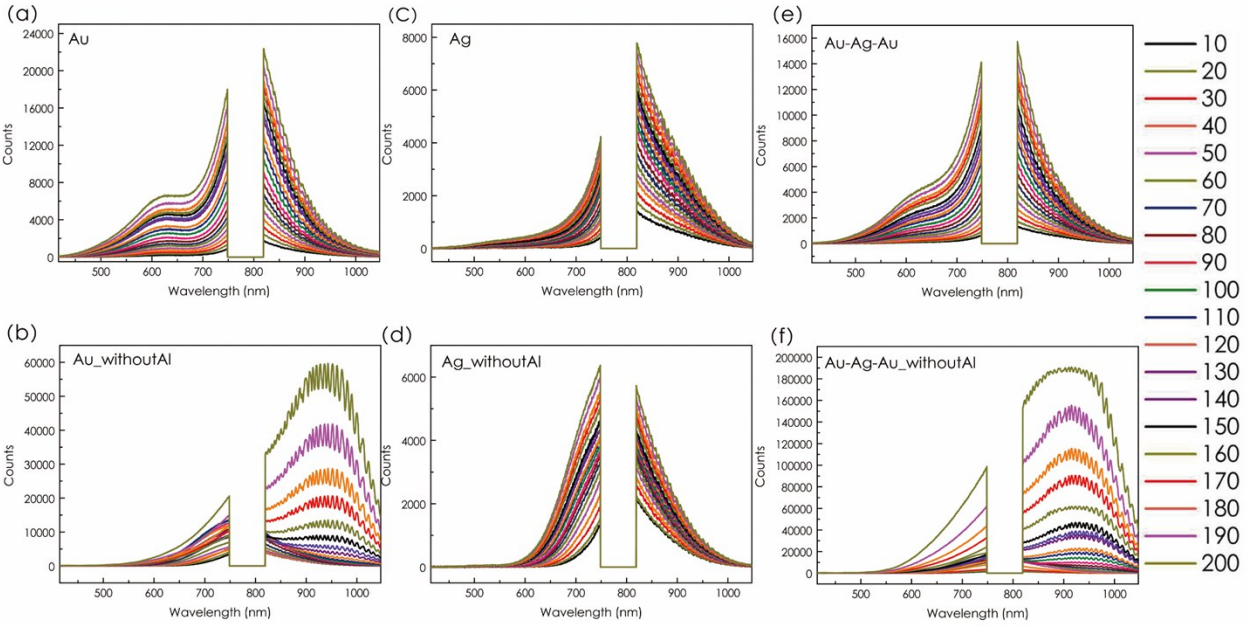

Figure S11. PL spectra of Au, Ag and Au-Ag-Au hybrid structures with the excitation power changing from 10 mW to 200 mW.

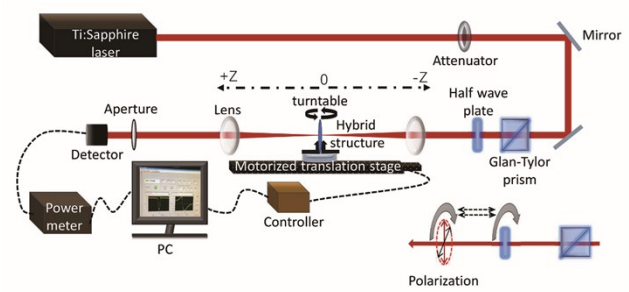

Figure S12. The schematic of Z-scan measurement setup.

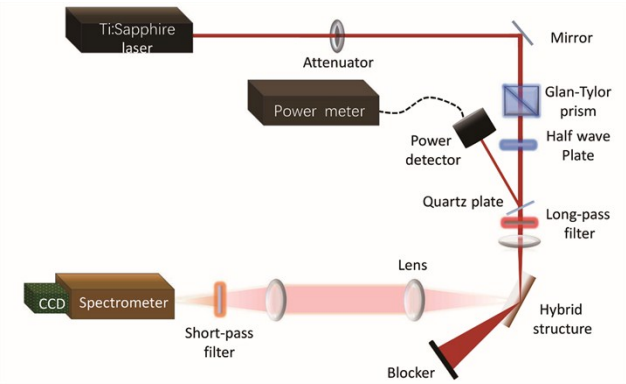

Figure S13. The schematic of SHG measurement setup.

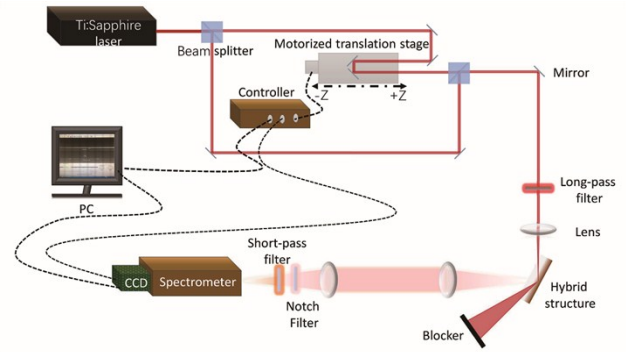

Figure S14. The schematic of supercontinuum lifetime measurement setup.

references

1. E. Hasman and V. Kleiner, 2014, **15**, 463-499.
2. S. Shen, L. Meng, Y. Zhang, J. Han, Z. Ma, S. Hu, Y. He, J. Li, B. Ren, T. M. Shih, Z. Wang, Z. Yang and Z. Tian, *Nano letters*, 2015, **15**, 6716-6721.
3. S. Chen, Y. Zhang, T. M. Shih, W. Yang, S. Hu, X. Hu, J. Li, B. Ren, B. Mao, Z. Yang and Z. Tian, *Nano letters*, 2018, **18**, 2209-2216.